Adsorption of Amino Acids on Oxide Supports: A Solid-State NMR Study of Glycine Adsorption on Silica and Alumina

ARTICLE *in* THE JOURNAL OF PHYSICAL CHEMISTRY C · OCTOBER 2009

Impact Factor: 4.77 · DOI: 10.1021/jp906891y

4 AUTHORS, INCLUDING:

Lingyu Piao
National Center for Nanoscience and Tech…
24 PUBLICATIONS **624** CITATIONS
SEE PROFILE

Lorenzo Stievano
Université de Montpellier, Montpellier, Fra…
132 PUBLICATIONS **1,663** CITATIONS
SEE PROFILE

Jean-François Lambert
Pierre and Marie Curie University - Paris 6
151 PUBLICATIONS **2,663** CITATIONS
SEE PROFILE

Adsorption of Amino Acids on Oxide Supports: A Solid-State NMR Study of Glycine Adsorption on Silica and Alumina

Irène Lopes, Lingyu Piao,† Lorenzo Stievano,‡ and Jean-François Lambert*

Laboratoire de Réactivité de Surface—UMR 7197 (CNRS), Université Pierre et Marie Curie, 4, place Jussieu, 75252 Paris Cedex 05, France

Received: July 21, 2009; Revised Manuscript Received: September 2, 2009

The adsorption of glycine on a well-characterized silica surface was investigated at the molecular level by means of solid-state ^{13}C and ^{15}N NMR spectroscopy, combined with macroscopic level information such as adsorption isotherms, pH dependence, or TGA. At least three different forms of glycine were observed and could be distinguished on the basis of their NMR properties: two bulk crystalline forms (α- and β-glycine, both containing the amino acid in the zwitterionic form) and a molecularly adsorbed glycine species. The latter is formed by adsorption of zwitterionic glycine to the silica surface through the formation of cooperative hydrogen-bond networks in a kind of molecular recognition phenomenon, yielding a glycine/surface adduct. In addition, crystallites of metastable β-glycine nucleate at the silica/solution interface already during the initial adsorption, in a phenomenon of surface-induced precipitation. On γ-alumina, glycine does not form well-defined adducts but may coordinate the Al^{3+} ions upon thermal activation.

Introduction

The adsorption of amino acids on inorganic oxide surfaces has been the object of many experimental studies, which were recently reviewed.[1] Among several others, our research group contributed to this knowledge with experimental studies that aimed at understanding adsorption mechanisms of glycine on silica.[2,3] In these studies, mostly on the basis of vibrational spectroscopy, we concluded that at low amino acid loadings there exists a molecularly adsorbed form of glycine interacting with specific surface sites (silanols, silanolates, or groups thereof) in a well-defined manner. The adsorption mechanism did not seem to involve the formation of covalent bonds, but rather of a specific pattern of hydrogen bonds with the surface. Subsequent investigations by molecular modeling agreed with the latter finding,[3−8] suggesting that glycine molecules may indeed be stabilized by specific hydrogen-bond structures involving silanols, silanolates, and H_2O molecules (the latter when adsorption is carried out in conditions of high water activity).

Since the experimental evidence with which to compare modeling results is still scant, additional independent sources of information on adsorbed amino acids molecules would be welcome. Solid-state NMR, in particular ^{13}C, immediately comes to mind as it has long been used as a characterization tool for amino acids, in particular glycine, in the solid state,[9−19] and to a lesser extent in the adsorbed state.[20−23] In the case of bulk glycine, ^{13}C NMR is sensitive to polymorphism in the solid state.[24] In fact, bulk glycine is known to crystallize as three polymorphs (not including others found only in extreme conditions), α-, β-, and γ-glycine. All three polymorphs contain glycine in the zwitterionic state, and the local environments of these zwitterions differ only by their specific arrangement of the H-bonds.

While the γ form is the most stable thermodynamically,[25] its formation is kinetically impeded. Crystallization from water solutions most often gives the α-polymorph, while the β-polymorph is obtained from other solvents, mixtures with low water activity, or recrystallization from the gas phase;[26] aging of β-crystals in moist air results in the slow transformation into the α-phase. Crystallization from octanoic acid emulsions gives β-crystals with special morphologies, e.g., dendritic and/or porous.[27] Crystallization on engineered thiols/gold surface can induce the preferential nucleation of α-, β-, or γ-glycine, depending on the gold island size and the pH;[28,29] coprecipitation of several crystalline forms is, however, the frequent outcome of such experiments. The application of intense electric fields through laser pulses causes the β-form to nucleate from water solutions instead of the α-form.[30] These and other examples[27,31] demonstrate that the control of glycine polymorphism is indeed the focus of active research interest, as it is considered a model system for more complicated instances of biochemical crystal engineering.

In our previous study on glycine adsorption, we reported that when the equilibrium glycine concentration in solution is higher than about 0.07 M, precipitation of bulk glycine crystals is observed by XRD in addition to molecular adsorption, even though the bulk solution is far below saturation levels; moreover, it is the β-polymorph of glycine that is generally observed, instead of the supposedly more stable α one. Similar observations were previously reported by El-Shafei et al. in glycine/boehmite adsorption experiments.[32] It appears therefore that precipitation in the presence of surfaces could constitute an additional tool to control amino acids polymorphism, but powder XRD, the technique most suited to study crystals polymorphism, cannot be applied effectively to the initial stages of precipitation where bulk amino acids would constitute a very minority phase as compared to the oxide support.

In order to understand more precisely the interactions of glycine and silica, leading either to specific adsorption mech-

* Corresponding author. E-mail: jean-francois.lambert@upmc.fr.

† Current affiliation: National Center for Nanoscience and Nanotechnology of China, Zhongguancun North First Tiao No. 11, 100190, Beijing, PR China.

‡ Current affiliation: AIME—Institut Charles Gerhardt, UMR 5253 CNRS, Université de Montpellier 2, Place Eugène Bataillon, F-34095 Montpellier Cedex 5, France.

10.1021/jp906891y CCC: $40.75
Published on Web 09/24/2009

TABLE 1: ^{13}C and ^{15}N Chemical Shifts Observed for Different Forms of Glycine[a] and of Glycine Dimers[b]

	α-glycine	β-glycine	γ-glycine	sodium glycinate	glycinium chloride	DKP	Gly-Gly
$^{13}COOH$ δ (ppm)	176.4	175.4	174.5	182.2	172.6	169.05	167.7 (amide) 173.05 (carboxylate)
$^{13}COOH$ T_1[c]	17.8 s	13.4 s	nd	nd	nd	nd	nd
$^{13}CH_2$ δ (ppm)	43.6	43.4	42.5	46.1	41.8	44.8	44.9 40.4
$^{15}NH_2$	−346.6	−347.5	−346.1	−361.5	−341.8	−274.4	−269.4 (amide) −359.45 (ammonium)

[a] Zwitterionic (α, β, γ), cationic (glycinium chloride), and anionic (sodium glycinate). [b] Cyclic dimer, diketopiperazine (DKP), and linear glycylglycine (Gly-Gly). [c] ^{13}C spin−lattice relaxation times are also reported for the carboxylate group.

anisms or to the precipitation of the β-polymorph of glycine in the vicinity of silica surfaces, we present here a solid-state ^{13}C and ^{15}N NMR spectroscopy investigation of glycine deposited on silica from solution with increasing glycine concentrations. This spectroscopic technique provides specific static and dynamic information on the two investigated nuclei, allowing one to study adsorptions even at relatively low glycine concentrations if isotopically enriched glycine molecules are used.

Experimental Section

1. Bulk Compounds. α-Glycine (99%) was directly purchased from Sigma-Aldrich. The other two polymorphs were prepared along generally accepted procedures.[33]

β-Glycine was obtained by rapid addition of methanol to a saturated aqueous solution of glycine, which was prepared by dissolving the appropriate amount of α-glycine in distilled water; the solid was then separated by filtration, dried in vacuo at room temperature, and stored in a desiccator.

γ-Glycine was prepared by adding a concentrated solution of NaOH to a saturated aqueous solution prepared from commercial α-glycine; the solid was initially obtained by evaporation of the solution at 70 °C and then dried in vacuo at room temperature for 24 h.

Sodium glycinate was a commercial product from Sigma-Aldrich. Diketopiperazine (DKP), the cyclic dimer of glycine, as well as the linear dimer Gly-Gly were provided by Bachem. Both 99% ^{13}C carboxylate-enriched glycine and 98% ^{15}N-enriched glycine were Isotec products.

The crystal structure and purity of all samples were checked by X-ray powder diffraction (XRD).

2. Adsorption Procedure. In a typical adsorption experiment, 300 mg of silica (Degussa Aerosil 380, BET surface area of 380 ± 20 m^2/g determined by N_2 physisorption at 77 K, PZC = 2.0) is immersed in 10 mL of an aqueous solution of glycine of the suitable concentration and stirred at room temperature for 4 h. The solid is then separated from the glycine solution by filtration and washed once with 10 mL of distilled water for 1 min. The washing solution is also eliminated by filtration and the solid dried in vacuo at room temperature.

For the experiments carried out at variable pH, the pH of the solutions are adjusted by adding appropriate amounts of aqueous solutions of H_3PO_4 or NaOH. In general, the solid samples will be noted as Gly/SiO_2 *x*M pH*y*, where *x* refers to the initial glycine concentration in the adsorption solution (in $mol \cdot L^{-1}$) and *y* refers to the adsorption pH (specification omitted when the pH was not adjusted).

In order to obtain an adequate signal-to-noise ratio in the ^{13}C NMR spectra on low-loading samples, the related adsorption experiments were carried out using glycine 99% ^{13}C-enriched on the carboxylate (Sigma-Aldrich).

3. NMR Spectroscopy. Solid-state ^{13}C and ^{15}N MAS NMR spectra were recorded at room temperature with a Bruker Avance 400 spectrometer with a field of 9.4 T, equipped with a 4 mm MAS probe with a spinning rate of 12−14 kHz.

^{13}C NMR spectra were obtained using a proton cross-polarization (CP) sequence with a pulse length of 3 μs (for a π/2 pulse of about 6.3 μs), a data acquisition time of 154 ms, and a recycle delay of 5−10 s. The effect of variable cross-polarization contact times (t_c) on the different observed signals was studied. The chemical shifts were determined by reference to an external adamantane sample ($\delta = +38.52$ ppm). The number of coadded transients was between 8 and 128 for pure reference compounds and from 10 000 to 14 400 for glycine/silica samples. The decoupling method was a two-pulse phase modulation scheme ($\phi = 15°$, decoupling frequency 50 kHz). Occasionally, a simple one-pulse (with high-power decoupling) sequence was used instead of CP, but longer recycle delays were needed in this case. Longitudinal relaxation times (T_1) values were measured using the SATREC pulse sequence.

^{15}N NMR spectra were also obtained with proton CP. The following parameters were used in this case: pulse length, 3.2 μs; data acquisition time, 44 ms; recycle delay, 5 s; cross-polarization contact time, 5 ms. The external chemical shift reference was α-glycine itself, as in ref 15.

Results

As expected, the ^{13}C CP/MAS NMR spectrum of glycine has peaks in two different regions: the signals between 42 and 44 ppm correspond to the methylene group, whereas those between 170 and 178 ppm correspond to the carboxylate group. The ^{15}N spectrum, on the other hand, presents a single peak between 341 and 362 ppm, corresponding to the amine group. As will be discussed hereafter, the observed ranges of ^{13}C and ^{15}N chemical shifts are useful to assess not only the protonation state of glycine but also to study the hydrogen-bonding networks by which the molecule is surrounded.

1. Bulk Glycine Polymorphs and Reference Compounds. Table 1 shows the solid-state ^{13}C and ^{15}N chemical shifts of the bulk glycine polymorphs and of other reference compounds in the carboxylate and methylene regions, obtained by CP/MAS experiments, except for the glycinate form, the spectrum of which was obtained by a HP/DEC experiment. The reproducibility of the chemical shifts is better than 0.05 ppm. The carboxylate region of the ^{13}C NMR spectra of these samples is shown in Figure 1.

The data in Table 1 show that zwitterionic glycine ($^+H_3N-CH-COO^-$) can easily be distinguished from both the cationic ($^+H_3N-CH-COOH$) and the anionic ($H_2N-CH-COO^-$) forms in both ^{13}C and ^{15}N NMR spectra. For the carboxylate signal, the ^{13}C isotropic chemical shift changes are from +1.9 to +3.8 ppm when going from the cation to the

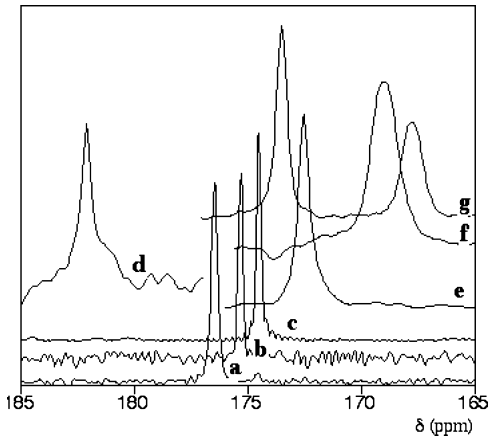

Figure 1. ^{13}C MAS NMR spectra in the carboxylate region of the glycine polymorphs and other reference compounds: (a) α-glycine, (b) β-glycine, (c) γ-glycine, (d) sodium glycinate, (e) glycinium chloride ("glycine hydrochloride"), (f) diketopiperazine (DKP), (g) glycylglycine (Gly-Gly).

zwitterion (depending on which zwitterionic polymorph is used for comparison) and from +5.8 to +7.7 ppm when going from the zwitterion to the anion. The direction (upfield shift upon protonation) and order of magnitude of these changes are comparable to those observed, for example, for histidine in the solid state[34] or in general for amino acids in aqueous solutions.[35] Note that, counterintuitively, the protonation of the carboxylate group affects the ^{13}C chemical shift of the carboxylate less than the protonation of the amino group.

Furthermore, it is seen that intermolecular interactions, e.g., hydrogen bonding, play an important role in the observed variations in chemical shifts. This is proved by comparing the ^{13}C chemical shifts in the same region of the three polymorphic forms of glycine (α, β, and γ), which all contain zwitterions and differ only in the arrangement of H-bonds between them. The signals of these three forms are well separate from each other, with observed chemical shifts very close to those previously published by Potrzebowski et al.[11] and Taylor.[14] The variation in chemical shifts gives an idea of what is expected from glycine forms differing in H-bonding patterns, which will be relevant in assessing the adsorption mechanism.

These values can be compared to those of two reference compounds obtained by the dimerization of glycine: Gly-Gly, the linear dimer of glycine obtained by the formation of one peptide bond, and diketopiperazine (DKP), the cyclic dimer of glycine in which two peptide bonds are formed. The signal of the amide group carbon in these two compounds is shifted upfield by several ppm respective to all COO^- and COOH signals, so that the eventual formation of amide bonds can be easily evidenced.

The difference in methylene chemical shifts in reference compounds is less marked and does not allow unambiguous discrimination of zwitterions with different H-bonding patterns. However, the chemical shifts of methylenes neighboring a carboxylate or carboxylic acid group are linearly correlated to those of the COO^- (or COOH), whereas methylenes neighboring an amide carbonyl do not follow the trend.

In the case of ^{15}N NMR spectra, the observed values of chemical shift for α- and γ-glycine agree with those previously reported by Kimura et al.[12] Compared to ^{13}C, even larger variations are measured for ^{15}N chemical shifts, which decrease by 4.3−5.7 ppm on going from the cationic to zwitterionic forms and by 15.4−14.0 ppm on going from the zwitterions to sodium glycinate, giving a global range of about 20 ppm. In this case, the effect of protonation is a displacement of the chemical shift toward low fields, contrary to what is observed for ^{13}C. Considering the large range of shifts available for ^{15}N, however, the values of chemical shifts for the three polymorphs of zwitterionic glycine appear all very close to each other compared to the differences observed for the ^{13}C values. Globally, the following order of chemical shifts is observed: δ(glycinate) < δ(β-gly) < δ(α-gly) < δ(γ-gly) < δ(glycinium), giving an overall anticorrelation between ^{13}C and ^{15}N shifts, with α glycine being only slightly aberrant (cf. infra). ^{15}N NMR is also highly sensitive to the formation of amide bonds, a phenomenon that is not treated in detail here but occurs upon mild thermal activation.[3−8]

While both ^{13}C and ^{15}N chemical shifts are coherent with published data, the data are surprising in other respects, particularly in the case of ^{13}C NMR spectroscopy. First, β-glycine is usually reported to be highly unstable in air, particularly if not kept under dry conditions,[36] and in a previous study it was reported to readily transform into α-glycine in the NMR rotor during data acquisition.[14] In our hands, the ^{13}C NMR spectrum of a sample aged for 24 h was exactly superimposable to the one of the fresh sample, and the polymorphic transition took several months for samples kept in vials under air. It is quite likely that the polymorphic transition occurs via surface dissolution/reprecipitation and thus is strongly dependent upon the atmospheric humidity, in agreement with the results of Drebushchak et al.[37] It remains advisible, therefore, to use β-glycine as soon as possible after preparation and, if necessary, to store it under dry conditions.

It has been reported that the ^{13}C spectrum of β-glycine is hardly observable in CP-MAS conditions, due to its unfavorable relaxation properties.[14] In fact, CP signals strongly depend on the contact time, which has to be optimized experimentally. The problem is not trivial and has been discussed before,[13,38] including in the case of bulk glycine[18] and the related alanine.[39] For the carboxylate carbon, which does not directly bear a hydrogen, an approximate formula for the evolution of signal intensity (I) as a function of experimental CP contact time (t_c) is, according to Sen et al.[39]

$$I = I^{\circ}\left(1 - \frac{T_{CH}}{T_{1\rho}}\right)^{-1}\left(e^{-t_c/T_{1\rho}} - e^{-t_c/T_{CH}}\right) \qquad (1)$$

Although this expression may be misleading in general for powder samples,[18] it has shown a satisfactory fit for the carboxylate carbon. The maximum intensity I° can only be approached if the $\{^1H-^{13}C\}$ polarization transfer characteristic time T_{CH} is much smaller than the rotational frame relaxation time for hydrogen, $T_{1\rho}$.

We have measured the evolution of signal intensities with $\{^1H-^{13}C\}$ contact time t_c for α-glycine and β-glycine (Figure 2). In the case of the α-glycine sample with the carboxylate enriched in ^{13}C, we observed a monotonic increase up to a contact time of 1 ms, followed by a rather slow decrease, for all practical purposes a plateau up to $t_c = 10$ ms. In the case of natural abundance α-glycine, the polarization buildup appeared to be slower, with a shorter plateau (cf. Figure 2 a); the polarization increase can be fitted with eq 1 were $T_{CH} = 0.37$ ms, but the fit is bad in the region of polarization decrease. This evolution is very similar to that observed by Taylor et al. working with a field of 7.05 T.[18]

In the case of natural abundance β-glycine (see Figure 2b), the maximum intensity is obtained after approximately 1 ms

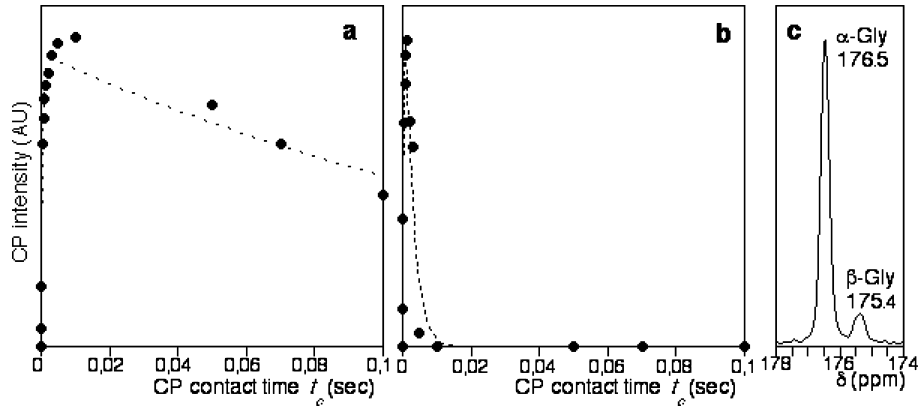

Figure 2. Variation of the intensity of the carboxylate signal with the $\{^1H-^{13}C\}$ contact time for α-glycine (a) and β-glycine (b). The dotted lines are the best fits of eq 1. (c) ^{13}C NMR spectrum (carboxylate region, $t_c = 1$ ms) of an equimolar mixture of α-glycine and β-glycine.

and then drops quickly; eq 1 gives a reasonably good fit of this evolution with $T_{CH} = 0.4$ ms and $T_{1\rho} = 2.4$ ms.

It follows that when performing ^{13}C CP-MAS NMR experiments on samples containing glycine, the setting of the $\{^1H-^{13}C\}$ contact time becomes a crucial parameter: in our conditions, a contact time in excess of 5 ms will selectively suppress any eventual β-glycine signal. Even if the contact time is set at the optimal value for β-glycine (i.e., about 1 ms), the relative amount of this form will be underestimated, as witnessed by the spectrum of an equimolar mixture of α- and β-glycine in Figure 2c, where the integrated signal of β-glycine is 8.6 times weaker than that of the α-form. In summary, although different forms of the amino acid can be detected simultaneously in a single sample, much care should be taken when trying to quantify them by the relative intensities of their ^{13}C CP-MAS signals. In contrast, it appears legitimate to discuss quantitatively the evolution of a given form in a series of samples, provided that the experimental acquisition parameters are exactly the same.

2. General Aspect of the Spectra for Gly/SiO_2 Samples. In general, typical ^{13}C spectra of SiO_2-supported glycine samples show three different signals in the carboxylate region, while ^{15}N spectra show three different signals in the ammonium region. In fact, two sharp lines at +176.5 and +175.4 ppm and a somewhat broader signal whose maximum is observed at a variable position between +170.8 and +174.5 ppm depending on the pH of the bulk solution are observed in the ^{13}C spectra. Similarly, two sharp peaks at −346.6 and −347.5 ppm and a broader one centered at about −349 ppm are observed in the ^{15}N spectra. XRD has shown that the Gly/SiO_2 samples with high glycine loadings contain bulk glycine phase(s) in addition to adsorbed species.[2,7] Accordingly, the peaks at +176.5 ppm (in the ^{13}C spectra) and −346.6 ppm (in the ^{15}N spectra) can definitely be assigned to bulk α-glycine, while those at +175.4 and −347.5 ppm, respectively, correspond to β-glycine.

For each nucleus, one signal cannot be assigned to any bulk form of glycine and tends to be broader than the other two; we assigned it therefore to a form of glycine interacting with silica surface groups, which we call "adsorbed glycine" for short. The existence of this distinct form is particularly evident if the ^{13}C and ^{15}N shifts are plotted against each other, as shown in Figure 3. The combination of ^{13}C and ^{15}N chemical shifts identifies this new form of glycine that is clearly out of the linear anticorrelation observed for the bulk forms. The ^{13}C spin−lattice relaxation time (T_1) of this new form is also significantly shorter than those of either α- or β-glycine, at 3.0 ± 0.7 s.

Finally, the ^{13}C magnetization buildup of adsorbed glycine in CP conditions is slower than for α-glycine, and a maximum

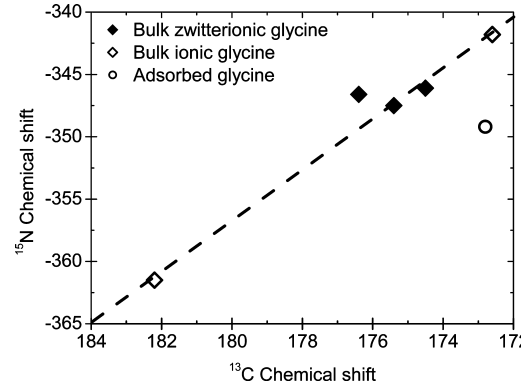

Figure 3. Comparison of ^{15}N and ^{13}C chemical shifts for the bulk and adsorbed forms of glycine. The dotted line shows the anticorrelation existing for the ^{13}C and ^{15}N chemical shifts for bulk glycine species.

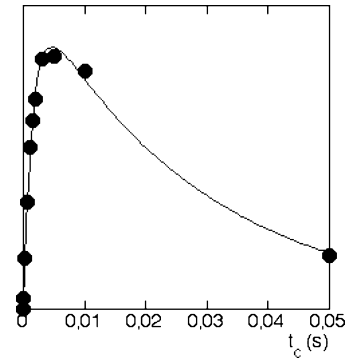

Figure 4. Variation of the intensity of the carboxylate signal with the $\{^1H-^{13}C\}$ contact time t_c for the adsorbed form of glycine. The curve is the best fit of eq 1.

is not reached until 5 ms contact time (Figure 4). The T_{CH} value (1.5 ms) is higher than in bulk forms of glycine, which is probably due to faster motions of some molecular group(s) in the adsorbed glycine; this might be put on a quantitative basis by carrying out variable-temperature experiments, although the task is not straightforward.[40] As for $T_{1\rho}$, it was found equal to 28.5 ms: the situation is intermediate between the cases of bulk α- and β-glycine, meaning that adsorbed glycine will be underestimated by CP-MAS with respect to α-glycine when both are present, but not as much as β-glycine is.

3. Dependence of ^{13}C NMR Signal on Glycine Loading. ***a. Natural Abundance Samples.*** In Gly/SiO_2 samples prepared at pH 6−7 from solutions of natural abundance glycine with different concentrations, we observed the three signals mentioned above (Figure 5). Although the signal-to-noise ratio is

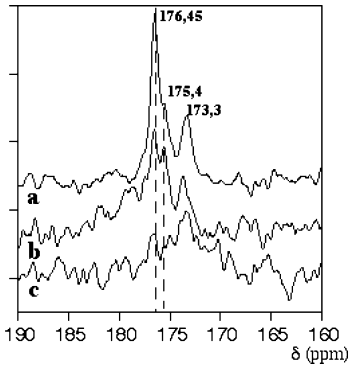

Figure 5. Natural abundance ^{13}C CP-MAS NMR spectra of Gly/SiO_2 samples prepared from different initial glycine concentrations, CP t_c = 5 ms;(a) Gly/SiO_2 0.3M, (b) Gly/SiO_2 0.15M, (c) Gly/SiO_2 0.07M. The dotted lines indicate the chemical shifts of reference α- and β-glycine. The spectra are normalized for NS (number of scans) and sample mass.

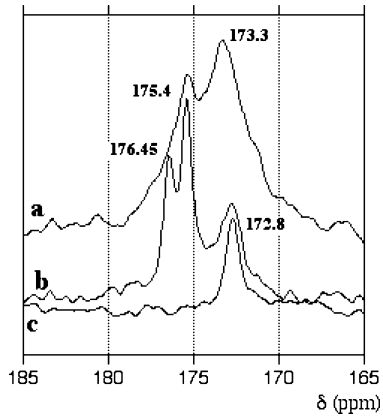

Figure 6. Effect of glycine loading on the ^{13}C CP-MAS NMR spectra of Gly*/SiO_2 samples: (a) Gly*/SiO_2 0.03M, contact time t_c = 5 ms; (b) same sample but with t_c = 1 ms; (c) Gly*/SiO_2 0.01M, t_c = 1 ms. The spectra are normalized for NS (number of scans) and sample mass.

rather poor, it is clear that when the loading decreases, the signals at +176.45 and +175.4 ppm progressively decrease, whereas the one at about +173 ppm remains present with approximately the same intensity.

In samples containing low glycine loadings, the presence of bulklike glycine is uncertain due to the poor signal-to-noise ratio. In order to obtain acceptable spectra also for these samples, 99% ^{13}C-enriched glycine (denoted Gly*) was used for their preparation.

b. ^{13}C-Enriched Samples. The spectra in the carboxylate region of samples Gly*/SiO_2 0.03M and Gly*/SiO_2 0.01M are shown in Figure 6. In the case of Gly*/SiO_2 0.03M, the spectrum was run first with a contact time of 5 ms as for the natural abundance samples (Figure 5a) and then in conditions that enhance the signals of bulk glycine (CP with t_c = 1 ms, Figure 5b). The same three signals as in Figure 1 are observed: α-glycine, β-glycine, and adsorbed glycine. In this sample, adsorbed glycine must be quantitatively predominant, but recording the spectrum with a low t_c value obviously leads to an underestimation of its importance.

For Gly*/SiO_2 0.01M, there is no trace of the bulk glycine polymorphs, even though the conditions were chosen to magnify their response, whereas the adsorbed glycine is present with an intensity very close to that of Gly/SiO_2 0.03M.

Bulk glycine forms thus appear to be present for all but the lowest-loading samples. Molecularly adsorbed glycine is present

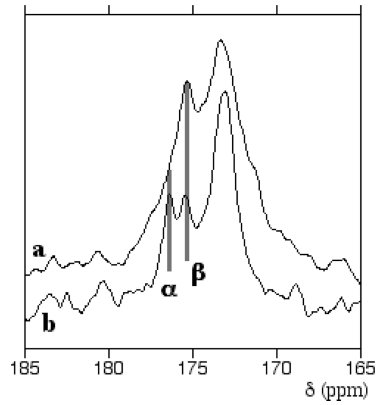

Figure 7. Effect of aging on ^{13}C NMR signal: (a) freshly prepared Gly*/SiO_2 0.03M; (b) same sample, aged for 1 year (t_c = 5 ms in both cases).

in all the studied samples, and as far as quantification is possible, its signal reaches a maximum value even for low glycine concentrations in the adsorption solution, corresponding to low loadings. The intensity of this signal does not increase significantly with increasing glycine concentrations, the additional glycine being instead present as bulk crystals. As we have said, it is not possible to provide an estimate of the relative contributions of bulk and adsorbed glycine in a given sample due to the different CP responses; in fact, exploratory attempts at recording single-pulse spectra suggest that even for the higher t_c value, the relative contribution of the adsorbed form is still underestimated.

For similar reasons, we will not attempt to quantify the distribution between the two bulk forms (α and β), but we can study the relative kinetic stabilities. Figure 7 shows the evolution of the signal of Gly/SiO_2 0.03 M upon aging for 1 year in ambient air. The α/β-glycine ratio manifestly increases, even though the β-form is still present even after this long period of time, while the adsorbed form is apparently unaffected. We can thus say that, in our solid samples, α-glycine remains thermodynamically preferred with respect to β-glycine. However, β-glycine is kinetically stabilized since the time scale of transformation to the α polymorph is of several months.

4. Acido−Basic Speciation of Adsorbed Glycine and ^{13}C NMR Spectroscopy. ***a. Influence of Adsorption pH in Low-Loading Samples.*** In a separate series of experiments, the behavior of adsorbed glycine as a function of the pH of the adsorption solution was studied on samples prepared by using 0.03 M aqueous solutions of ^{13}C-enriched glycine, corresponding to low overall glycine loadings. As seen on Figure 8, molecularly adsorbed glycine is present in all samples, but the corresponding peak shifts downfield with increasing solution pH. Bulk forms of glycine are only apparent at intermediate pH values, and β-glycine only at pH 5−7.

Figure 9 plots the ^{13}C chemical shift (δ) of molecularly adsorbed glycine as a function of equilibrium solution pH. There is a definite pH step, although it is not as sharp as would be expected for the existence of a fast equilibrium between the protonated and deprotonated forms of an acid−base couple; this point will be dealt with in the Discussion. The chemical shifts of three solid reference compounds (two containing the zwitterion $HGly^{\pm}$, one the cation H_2Gly^+) are indicated as horizontal lines for comparison.

b. Influence of Adsorption pH in High-Loading Samples. Control experiments were carried out on samples prepared from unmarked glycine. Due to the lower signal intensity, higher glycine loadings were desirable, which was achieved by using

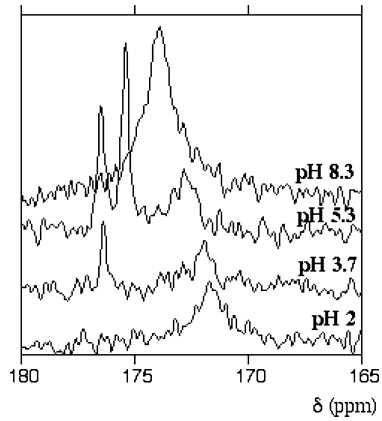

Figure 8. ^{13}C CP/MAS NMR spectra of Gly*/SiO_2 0.03M samples; effect of the final pH of the bulk solution on the NMR spectrum of adsorbed glycine ($t_c = 1$ ms). Spectra are normalized for NS (number of scans) and sample mass.

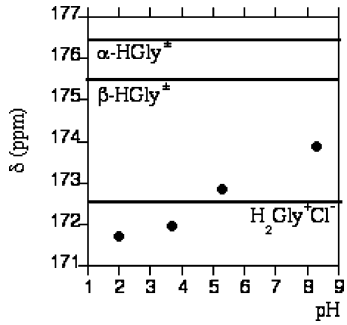

Figure 9. Evolution of the chemical shift of molecularly adsorbed glycine with the pH of the adsorption solution; comparison with chemical shifts of reference compounds.

a glycine concentration in the starting solution of 0.30 M. In most of the pH range, the same three signals already discussed were present: β-glycine was observed between pH 4 and 8, and α-glycine between pH 4 and 9. The signal of adsorbed glycine was present from pH 2 to 8, but it was considerably less intense with respect to the bulk forms than in the low-loading samples, as expected.

At high pH values (9 and 10), a signal at +174.5 ppm was predominant; this may be due to the deprotonated form of the adsorbed glycine (see preceding paragraph), but in view of the relatively high intensity and sharpness, it could also be attributed to the precipitation of some bulk γ-glycine form. This would be in keeping with the observations of Lee et al.,[29] indicating that γ-glycine forms preferentially in rather basic or rather acidic solutions.

The $-CH_2-$ peak could be observed in addition to the $-COO^-$ peak for natural abundance, high-loading systems, and its evolution was compatible with that of the signals in the carboxylate range. We observed a first $-CH_2-$ signal at 44.0 ppm, which corresponds with the bulk glycine, and another one shifted downfield (44.4−44.9 ppm), corresponding to molecularly adsorbed glycine.

5. Quantification of the Adsorption from Macroscopic Data. As we have seen, quantification of adsorbed amounts from NMR data is not straightforward (we have semiquantitatively discussed the relative amounts of different forms of glycine on silica but made no attempt at absolute quantifications). In colloid chemistry studies, adsorbed amounts are usually determined by analysis of the amounts remaining in solution after reaching the adsorption equilibrium: the differences with the initial concentrations corresponds to the adsorbed amounts, and plotting these as a function of the equilibrium concentrations gives the "adsorption isotherm". An adsorption isotherm of glycine on silica at natural pH (6) is shown in Figure 10.

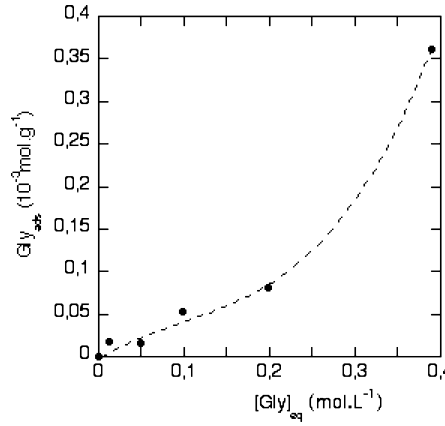

Figure 10. Adsorption isotherm for Gly/SiO_2 pH6, from HPLC analysis of the adsorption solution.

In the case of colloidal silica, however, it is not possible to directly compare these amounts with the glycine contents of the solids after separation and drying. This is because phase separation procedures (e.g, filtration, centrifugation) do not allow the recovery of the solid silica alone, since a strongly hydrated gel-like material retaining a substantial amount of water solution is usually obtained. In our case, in spite of the nonporous nature of the silica, 1 g of silica retained about 2.67 g of water solution, and since this solution contains nonadsorbed glycine, an additional amount of glycine equal to $2.67 \times 10^{-3}x$ mmol·(g of SiO_2)$^{-1}$ was physically retained (where x is the molar concentration of glycine in the equilibrium solution) and was therefore still present after drying. Since our main interest was in specifically adsorbed glycine, a washing step was applied in the hope of partly removing this physically retained glycine. This would still leave a minor amount of physically retained glycine, but it would fall to $1.87 \times 10^{-4}x$ mol·g^{-1} for perfect dilution upon washing, hopefully low enough not to obscure the signal of specifically adsorbed glycine.

There is actually a relatively easy way to obtain precise quantification of glycine in the solid phase obtained after drying, based on the analysis of differential thermogravimetric (DTG) patterns. This has been discussed in our previous study,[2] where typical DTGs may also be found. Any additional glycine found in the solid (by DTG) as compared to the adsorption isotherm (by HPLC) would correspond to glycine from the physically retained solution. Figure 11 provides an experimental estimate of this physically retained quantity, as $Q_{TG} - Q_{HPLC}$.

It can be seen that dilution of the physically retained glycine is not perfectly efficient under our conditions, especially for low concentrations, since the physically retained amount is intermediate between those expected without washing and with perfect washing. The efficiency might possibly be increased by using longer washing times, but one would then run the risk of reversing the molecular adsorption, too (vide infra). There is no satisfactory way out of this quandary.

6. Glycine Speciation Changes upon Washing. ^{13}C NMR may be applied to try and understand the qualitative effects of washing, although it must be kept in mind that a drying step always has to be applied before NMR characterization.

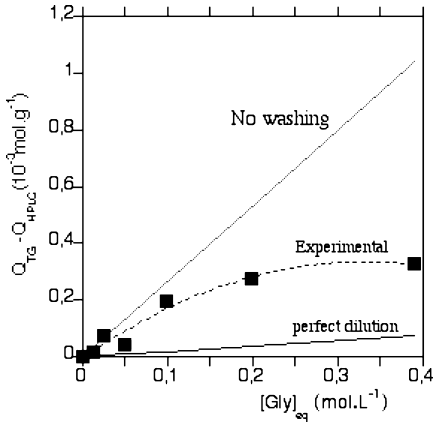

Figure 11. Comparison between glycine amounts in the final dry solids obtained by thermogravimetric analysis (Q_{TG}) and amounts adsorbed from the solution obtained by HPLC (Q_{HPLC}). The dotted line is a simple optical guide.

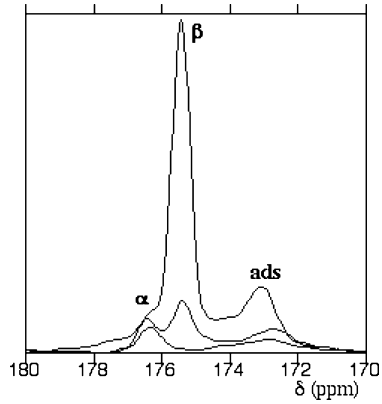

Figure 12. ^{13}C NMR of Gly/SiO_2 0.03M. From top to bottom: unwashed, washed once, washed twice. CP contact time, 1 s. Spectra normalized for the number of scans.

Figure 12 compares the spectra of three samples prepared from 0.3 M glycine solutions at natural pH: (a) dried without washing, (b) dried after one washing, and (c) dried after two washings.

Both bulk and adsorbed forms are observed in the three spectra, but their evolution upon washing is different.

In unwashed Gly/SiO_2 a large amount of bulk glycine is present, overwhelmingly as the β-form, while α-glycine is only present in trace amounts. The β-form is strongly reduced after one washing, and has disappeared altogether after two washings. This may be partly due to preferential dissolution, but the $\beta \rightarrow$ α polymorphic transition, which is expected to occur in wet environments,[37] must also be occurring since the amount of α-glycine actually increases. Concerning the signal of adsorbed glycine, its position shifts by a few tenths of a ppm (at most 0.3 ppm) and its intensity also decreases upon washing, but by factors smaller than for bulk glycine. These integrated intensities of each signal are provided in Table 2. Recall that the signal decompositions do not provide exact estimates of the amounts of the different forms; however, the quantitative evolution of each signal in a series of spectra is meaningful.

7. Comparison with Gly/Al_2O_3. The ^{13}C NMR signals of glycine deposited on alumina (Figure 13) are much broader than for glycine on silica. The carboxylate signal is centered at +177 ppm, close to the α-glycine signal. However, no bulk forms of glycine are observed by XRD. In view of the broadening, it is difficult to say if the resonance is significantly shifted with respect to bulk glycine. In addition, the methylene peak is also

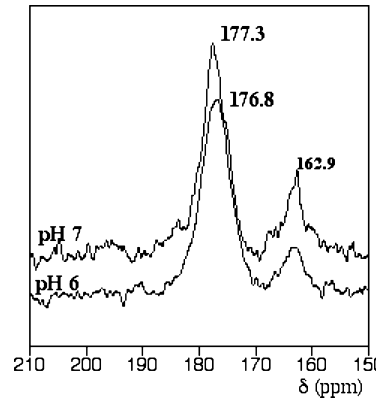

Figure 13. ^{13}C NMR of Gly/Al_2O_3 pH6 and Gly/Al_2O_3 pH7.

TABLE 2: Evolution of the Normalized Intensities of the CP-MAS NMR Signals (Arbitrary Units) Corresponding to the Various Forms of Glycine, as a Function of the Number of Drying Steps

	unwashed	washed once	washed twice
adsorbed glycine	24.7	11.2	9.7
β-glycine	75.3	12.4	0
α-glycine	traces	3.7	5.8

considerably broadened but in addition significantly shifted (observed at +40.9 ppm instead of +43.7 ppm).

It seems that the observed signal is heterogeneously broadened and represents the sum of contributions from glycine molecules interacting with several slightly different surface sites, in conformity with the well-known surface heterogeneity of γ-alumina surfaces in the presence of an aqueous phase.

The signal at +162.9 ppm is most probably due to surface carbonates at the surface of alumina, as evidenced by control experiments on glycine-free $(CO_3)^{2-}$/alumina systems prepared from a Na_2CO_3 solution; the latter show three components, one of which (+164.2 ppm) has the same width and approximately the same position as the signal under discussion. In addition, a similar signal has been assigned to carbonates by Yuan et al. in the aspartic acid/hydrotalcite system.[21] The carbonate signal is not significantly present in the starting alumina, but carbonate may be formed from atmospheric CO_2 during the amino acid deposition procedure, since no particular precautions were taken to isolate the suspension from air.

We attempted to deposit glycine by another procedure, chemical vapor deposition, to see if a better defined signal, possibly indicative of a more specific binding, could be obtained in this way. In fact (Figure 14), we obtained a composite signal with two components at 177.6 and 170.3 ppm. The latter signal was not present in Gly/Al_2O_3 from aqueous deposition and could therefore correspond to glycine adsorbed by a different mechanism that is specific of the CVD conditions.

Discussion

The first point to be underlined is the potential of solid-state MAS NMR to evaluate the in situ speciation of adsorbed amino acids. The Gly/SiO_2 system constitutes a case in point, since usual preparation procedures produce mixtures of three different forms: two bulk glycine phases and one molecularly adsorbed form. Our results, obtained on both ^{13}C or ^{15}N nuclei, confirm that simple NMR experiments allow one to discriminate these forms without difficulty. Quantitative estimates, on the other hand, are much trickier: as we showed for ^{13}C (^{15}N experiments raise the same issues) single-pulse NMR is not realistic in view

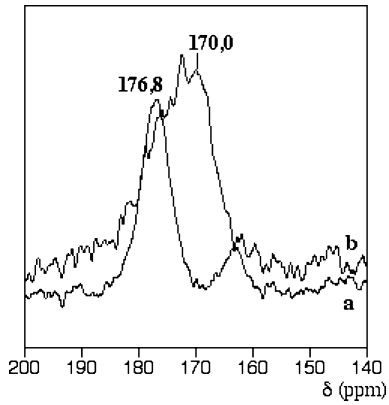

Figure 14. ^{13}C NMR of glycine/alumina prepared by adsorption from aqueous solutions (at pH 6, spectrum a) and by CVD (spectrum b).

of the large carbon T_1, and in CP the three forms have very different polarization responses as a function of time, and their contributions to the signal will never be proportional to their relative amounts in the sample. If the polarization contact time is optimized for a given form, the other forms will be underestimated, sometimes by more than 1 order of magnitude; furthermore, the maximum signal obtained along the polarization curve is scaled by an amount that depends on the $T_{CH}/T_{1\rho}$ ratio and will be different for each form. Finally, the simple expression that would allow in principle to correct the observed intensity of each signal is not strictly valid, at least in the case of natural abundance α-glycine. To summarize, attempts at quantifying the relative amounts of the different forms in a sample would necessitate a complete study of the relaxation behavior, a study whose conclusions would probably not remain valid beyond the sample under study. However, it is still possible to work in a semiquantitative way, e.g., to set the polarization contact time to such a low value as to enhance the response of the bulk forms, in which case NMR will detect them even if their amount is much too low to be revealed by XRD.

One of the signals observed in most Gly/SiO_2 samples was attributed to molecularly adsorbed glycine. By this we mean that glycine is engaged in a specific interaction with surface groups, one that results in a modification of the electronic density. The change in chemical shift with respect to the bulk zwitterionic forms is of the same order as the difference in δ between the polymorphs, suggesting a modification by H-bonding to the surface, rather than by the formation of a covalent bond which would result in at least twice larger shifts. This is in line with the conclusion of previous studies using other characterization techniques such as IR and molecular modeling (see introduction), indicating that the adsorption of amino acids on silica surfaces occurs through the formation of hydrogen-bond networks. Therefore, the molecularly adsorbed glycine form could be called a "surface adduct".

The width of the NMR signals also deserves some comments. Bulk crystalline glycine in reference samples has a full width at half-height (fwhm) of 0.23−0.34 ppm, and bulk glycine signals observed in Gly/SiO_2 samples are not different in this respect (fwhm = 0.26−0.39 ppm), indicating the lack of heterogeneous broadening and therefore well-crystallized bulk glycine particles. The glycine adduct on silica has an only slightly broader peak (fwhm 0.85−1.67 ppm), meaning that the H-bond interaction between glycine and the surface groups is quite well-defined. This is a rather surprising conclusion, because we are dealing with amorphous silica, a material that exhibits a wide variety of local environments and connectivities for the exposed silanols. It seems that glycine is able to select a rather uniform subset of these surface groups, giving rise to a specific interaction in a kind of molecular recognition. Actually, a similar conclusion was previously reached for the adsorption of several transition-metal complexes on the same silica, using a different probe of the molecular environment (UV−visible[41,42]). A slightly different possibility would be that glycine adsorption itself contributes to shape the molecular environment at the adsorption site, since the well-known flexibility of the Si−O−Si hinges allows some variation of the silanols groups positioning; in contrast, this would not be possible on alumina (vide infra).

In contrast, Gly deposited on alumina shows a very broad signal (fwhm = 5−6 ppm), which is not significantly shifted from bulk glycine. This is most likely heterogeneous broadening, due to the coexistence of many slightly different weakly adsorbed glycine molecules. On the other hand, when glycine is deposited on the alumina surface activated at moderate temperatures in CVD experiments, a new component appears in the signal at 170.0 ppm, i.e., with a larger displacement from bulk forms than in the SiO_2 case. According to the previous line of reasoning, this could indicate the formation of a covalent bond between glycine and the surface, and indeed, this appears chemically reasonable: surface Al^{3+} are bound to H_2O ligands under normal conditions at room temperature, while the thermal activation in CVD conditions will free them by evolution of gaseous water, so they can act as Lewis acidic sites toward glycine molecules. The signal at 170.0 ppm would then be due to Gly/Al^{3+} surface coordination compounds; while the details remain to be worked out, coordination of at least the carboxylate moiety to Al^{3+} is definitely a possibility.[43,44] To check this, we deposited glycine on an Al-pillared clay, a nanocomposite material including some easily dehydrated $Al^{3+}_{surf}-(OH_2)$ bonds on the surface of its pillars.[45] Here, too, a composite ^{13}C NMR signal is observed in the carboxylate region, with a component at +170 ppm.

Coming back to glycine on silica, which is the main focus of this paper, additional remarks can be made on both the adsorbed and the bulk forms.

The ^{13}C chemical shift of the adsorbed form is pH-dependent, and the range of values reported in Figure 9 seem to suggest that indeed two adsorbed forms in fast proton exchange are present, one cationic ($H_2Gly^+_{ads}$) and one zwitterionic ($HGly^{\pm}_{ads}$), in proportions depending on the pH of the adsorption solution. A few points must be noted here. First, the extreme values of the ^{13}C chemical shifts, corresponding in principle to $H_2Gly^+_{ads}$ and $HGly^{\pm}_{ads}$, do not exactly coincide with those observed for the reference compounds [H_2Gly^+ in glycinium chloride or $HGly^{\pm}$ in any of the glycine polymorphs (cf. Table 1)], so that the conclusion of a specific network of H-bonds with the surface of silica for the adsorbed form(s) remains valid. Finally, the chemical shift step is expected at the pK_a of the acid−base couple. Now the pH values correspond to those of the initial adsorption solution, not those of the washing solution which was equilibrated with the solid sample during the final washing step, which may account for the broadening of the pH step; nevertheless, its position still seems too high as compared to the known pK_a of the $H_2Gly^+/HGly^{\pm}$ in solution. Thus, it is likely that adsorption causes significant and measurable changes in the acido−basic properties of glycine.

Regarding the bulk forms of glycine, previous observation by powder XRD had evidenced their presence for equilibrium glycine concentrations in solution of about 0.075 M (recall that glycine solubility at room temperature is >3 M).[2] Now ^{13}C NMR reveals that the phenomenon is apparent for even lower glycine

activities, corresponding to bulk concentrations lower than 0.03 M. It is possible, but not demonstrated, that this precipitation starts already during the adsorption step, in the presence of the liquid phase. The fact that a given phase may precipitate in the presence of an oxide surface for concentrations significantly lower than the bulk solubility limit is a well-known phenomenon in geochemistry, where it is called "surface precipitation".[46,47] The upward concave shape of the adsorption isotherm in Figure 10 would be compatible with this idea, with the rising part at high concentrations corresponding to the growth of glycine crystallites on nuclei formed at lower concentrations.

However, it must be recalled that the solids submitted to NMR investigation are the end result of a procedure made of several steps. After the initial adsorption, the solid phase is separated from the supernatant by filtration, washed, and finally dried. The particular problem of working on high surface area silica is that this material retains a large amount of water that cannot be separated physically. Consequently, the gels collected at this stage contain in fact two sources of glycine: the adsorbed (and/or surface-precipitated) molecules and a "reservoir" not interacting with the surface, in the physically retained solution. As the sample is dried, molecules from the reservoir are forced either to precipitate or perhaps to interact individually with surface sites liberated by the emission of water molecules. Thus, the speciation observed by NMR is the result of a complex, two-step process. The intercalation of a washing step in our procedure was an attempt to simplify the speciation by reducing the glycine reservoir: as can be seen in Figure 11, it is not perfectly efficient in doing so, while Figure 11 shows that it introduces additional complications by inducing a $\beta \rightarrow \alpha$ polymorphic transition. Furthermore, repeated washings cause a slow decrease of the molecularly adsorbed form, indicating a fast reversibility of the adsorption process: we can thus surmise that the desorption reaction has a rather low activation barrier, which is in keeping with the adsorption mechanism being due to H-bonding and with the adsorption isotherm indicating a low affinity of the glycine molecules in aqueous solution for the surface of silica.

An additional major question is why metastable β-glycine is formed in preference to α-glycine, especially in the unwashed samples. In the region where bulk forms of glycine are most noticeable (pH 4−7), the surface of silica bears a significant negative charge, since its PZC is about 2. It therefore imposes an important electric field in the diffuse layer. The effects of such high electric fields are rather spectacular modifications of the solution close to the surface, as compared to bulk water: its density increases, its electric permittivity decreases, and it becomes generally more similar to an organic solvent.[48−50] It is not surprising, therefore, that many substances may see their solubility altered in the vicinity of a charged interface, explaining the surface precipitation phenomenon.

Regarding the preferential precipitation of β-glycine, it may be due to a more direct influence of the interfacial electric field. We have underlined in a previous publication that this field reaches values on the order of 10^8 V·m^{-1}, comparable to those imposed by laser pulses, which are known to cause preferential nucleation of β-glycine or "polarization switching" of the glycine structure.[30] Some publications have reported a "memory effect" in glycine precipitation, where solutions obtained from pure α-glycine crystals would be more prone to nucleate the α-form than solutions prepared from mixtures containing other polymorphs.[33] In fact, it has been suggested that "head-to-tail" dimers of glycine zwitterions may exist in pure water solutions and facilitate the nucleation of the α-glycine structure, where such packing arrangements are indeed found.[51,52]

The effect of charged surfaces we observe here would be compatible with this hypothesis, since intense interfacial electric fields would be expected to cause a realignment of the glycine zwitterions and thus to destroy the dimeric α-glycine nuclei, causing the preferential nucleation of the β-glycine structure. This may be compared with instances in which charged molecules or inorganic ions dissolved in the bulk have caused the formation of γ-glycine, which like β-glycine lacks the head-to-tail dimers.[51−53] However, it must be noted that the existence of the dimers in solution has recently been contested on the basis of freezing point depression measurements.[54] Therefore, the previous explanation may have to be rexamined, but it emphasizes the interest of studying the influence of surfaces on adsorbate structuration.

Conclusion

In glycine/silica samples prepared along standard colloidal chemistry procedures, a molecularly adsorbed form coexists with one or two forms of bulk glycine (α and/or β). All three forms can be detected simultaneously and differentiated by standard CP-MAS ^{13}C and ^{15}N NMR. Relative quantification, while not impossible in theory, is very difficult due to different polarization transfer properties.

The molecularly adsorbed glycine species probably interacts with the surface through a specific network of H-bonds, in agreement with information obtained from other techniques and from molecular modeling. In view of the dependence on adsorption pH, adsorbed glycine is probably involved in an acido−basic couple consisting of an adsorbed glycinium and the corresponding adsorbed cation ($H_2Gly^+_{ads}$/$HGly^{\pm}_{ads}$). At any rate, the NMR signal of the adsorbed forms is sharp, suggesting a well-defined surface complex and therefore the recognition of a specific subset of the surface silanols: not all Si−OH constitute potential sites for the formation of surface adducts with glycine.

Bulk glycine crystallites may nucleate from the more concentrated solutions already during the initial adsorption, i.e., at the silica/solution interface, in a phenomenon of surface-induced precipitation. More bulk glycine precipitates upon drying; the β-polymorph is formed initially, while the α-polymorph remains the more stable one in the long run. The surface might also inhibit the nucleation of α-glycine crystallites and slow down the transformation of β- to α-glycine.

A negative observation must be shortly commented here. The glycine/silica samples dried at room temperature show no evidence of peptide bond formation, which should be easily observed if present (see Figure 1 and corresponding discussion). This is relevant for prebiotic chemistry: it has long been thought that the original, abiotic polymerization of small biological molecules (such as amino acids to peptides), which is thermodynamically disfavored in solution, could have happened in the "adsorbed phase", and there are indications that polyglycine is formed in the presence of silica submitted to "wetting-and-drying" samples.[57] Our results suggest that no peptide bonds are formed unless the system is thermally activated; i.e., adsorption alone is insufficient to provide a prebiotic peptide formation scenario, which is in agreement with recent molecular modeling results.[58] We hope to discuss the matter in more detail in a forthcoming publication.

One final conclusion of the present study is that the practical details of glycine/silica samples preparation, i.e., the macroscopic deposition procedure, must be carefully optimized since

different procedure will cause different speciations of glycine at the molecular level. This caveat will be familiar to people working in the field of supported metal catalysts preparation and calls for the application of molecular characterization techniques at all successive steps of the glycine deposition procedure; for instance, initial speciation in the presence of the adsorption solution may be studied by ATR[55] and possibly by in situ liquid-state NMR.[56]

Acknowledgment. The authors are grateful to Jocelyne Maquet for help in the acquisition of ^{13}C NMR spectra. L.P. acknowledges a postdoctoral grant ("Accueil de Jeunes Chercheurs Étrangers") from the French Ministry of Research.

References and Notes

(1) Lambert, J.-F. *Orig. Life Evol. Biosphere* **2008**, *38*, 211.
(2) Meng, M.; Stievano, L.; Lambert, J.-F. *Langmuir* **2004**, *20*, 914.
(3) Stievano, L.; Piao, L.; Lopes, I.; Meng, M.; Costa, D.; Lambert, J.-F. *Eur. J. Mineral.* **2007**, *19*, 321.
(4) Lomenech, C.; Bery, G.; Costa, D.; Stievano, L.; Lambert, J.-F. *ChemPhysChem* **2005**, *6*, 1061.
(5) Rimola, A.; Tosoni, S.; Sodupe, M.; Ugliengo, P. *Chem. Phys. Lett.* **2005**, *408*, 295.
(6) Rimola, A.; Tosoni, S.; Sodupe, M.; Ugliengo, P. *ChemPhysChem* **2006**, *7*, 157.
(7) Costa, D.; Lomenech, C.; Meng, M.; Stievano, L.; Lambert, J.-F. *THEOCHEM* **2007**, *806*, 253.
(8) Rimola, A.; Sodupe, M.; Ugliengo, P. *J. Am. Chem. Soc.* **2007**, *129*, 8333.
(9) Andrew, E. R.; Hinshaw, W. S.; Hutchins, M. G. *J. Magn. Reson.* **1974**, *15*, 196.
(10) Malkin, V. G.; Malkina, O. L.; Salahub, D. R. *J. Am. Chem. Soc.* **1995**, *117*, 3294.
(11) Potrzebowski, M. J.; Tekely, P.; Dusausay, Y. *Solid State Nucl. Magn. Reson.* **1998**, *11*, 253.
(12) Kimura, H.; Nakamura, K.; Eguchi, A.; Sugisawa, H.; Deguchi, K.; Ebisawa, K.; Suzuki, E.-i.; Shoji, A. *J. Mol. Struct.* **1998**, *447*, 247.
(13) Kolodziejski, W.; Klinowski, J. *Chem. Rev.* **2002**, *102*, 613.
(14) Taylor, R. E. *Concepts Magn. Reson., A* **2004**, *22A*, 79.
(15) Gervais, C.; Dupree, R.; Pike, K. J.; Bonhomme, C.; Profeta, M.; Pickard, C. J.; Mauri, F. *J. Phys. Chem. A* **2005**, *109*, 6960.
(16) Zujovic, Z. D.; Bowmaker, G. A. *J. Magn. Reson.* **2006**, *181*, 336.
(17) Taylor, R. E.; Chim, N.; Dybowski, C. *J. Mol. Struct.* **2006**, *794*, 533.
(18) Taylor, R. E.; Chim, N.; Dybowski, C. *J. Mol. Struct.* **2007**, *830*, 147.
(19) Lee, J.-S.; Khitrin, A. K. *Concepts Magn. Reson., A* **2008**, *32A*, 56.
(20) Di Leo, P. *Clays Clay Miner.* **2000**, *5*, 495.
(21) Yuan, Q.; Wei, M.; Evans, D. G.; Duan, X. *J. Phys. Chem. B* **2004**, *108*, 12381.
(22) Reinholdt, M. X.; Kirkpatrick, R. J. *Chem. Mater.* **2006**, *18*, 2567.
(23) Reinholdt, M. X.; Babu, P. K.; Kirkpatrick, R. J. *J. Phys. Chem. C* **2009**, *113*, 3378.
(24) Stievano, L.; Tielens, F.; Lopes, I.; Folliet, N.; Gervais, C.; Costa, D.; Lambert, J.-F. Submitted 2009.
(25) Chongprasert, S.; Knopp, S. A.; Nail, S. L. *J. Pharm. Sci.* **2001**, *90*, 1720.
(26) Liu, Z.; Zhong, L.; Ying, P.; Feng, Z.; Li, C. *Biophys. Chem.* **2008**, *132*, 18.
(27) Nicholson, C. E.; Cooper, S. J.; Jamieson, M. J. *J. Am. Chem. Soc.* **2006**, *128*, 7718.
(28) Lee, A. Y.; Lee, I. S.; Dette, S. S.; Boerner, J.; Myerson, A. S. *J. Am. Chem. Soc.* **2005**, *127*, 14982.
(29) Lee, I. S.; Kim, K. T.; Lee, A. Y.; Myerson, A. S. *Cryst. Growth Design* **2007**, *8*, 108.
(30) Garetz, B. A.; Matic, J.; Myerson, A. S. *Phys. Rev. Lett.* **2002**, *89*, 175501.
(31) Weissbuch, I.; Torbeev, V. Y.; Leiserowitz, L.; Lahav, M. *Angew. Chem., Int. Ed.* **2005**, *44*, 3226.
(32) El Shafei, G. M. S.; Philip, C. A. *J. Colloid Interface Sci.* **1995**, *176*, 55.
(33) Boldyreva, E. V.; Drebushchak, V. A.; Drebushchak, T. N.; Paukov, I. E.; Kovalevskaya, Y. A.; Shutova, E. S. *J. Therm. Anal. Calor.* **2003**, *73*, 409.
(34) Henry, B.; Tekely, P.; Delpuech, J.-J. *J. Am. Chem. Soc.* **2002**, *124*, 2027.
(35) Surprenant, H. L.; Sarneski, J. E.; Key, R. R.; Byrd, J. T.; N.Reilley, C. *J. Magn. Reson.* **1980**, *40*, 231.
(36) Drebushchak, T. N.; Boldyreva, E. V.; Seretkin, Y. V.; Shutova, E. S. *Zh. Strukt. Khim.* **2002**, *43*, 899.
(37) Drebushchak, T. N.; Boldyreva, E. V.; Seryotkin, Y. V.; Shutova, E. S. *J. Struct. Chem.* **2002**, *43*, 835.
(38) Fyfe, C. A.; Brouwer, D. H.; Tekely, P. *J. Phys. Chem. A* **2005**, *109*, 6187.
(39) Sen, S.; Yu, P.; Risbud, S. H.; Dick, R.; Deamer, D. *J. Phys. Chem. B* **2006**, *110*, 18058.
(40) Fülber, C.; Demco, D. E.; Blümich, B. *Solid State Nucl. Magn. Reson.* **1996**, *6*, 213.
(41) Boujday, S.; Lambert, J.-F.; Che, M. *J. Phys. Chem. B* **2003**, *107*, 651.
(42) Boujday, S.; Lambert, J.-F.; Che, M. *ChemPhysChem* **2004**, *5*, 1003.
(43) Kubicki, J. D.; Blake, G. A. *Geochim. Cosmochim. Acta* **1996**, *60*, 4897.
(44) Persson, P.; Karlsson, M.; Öhman, L.-O. *Geochim. Cosmochim. Acta* **1998**, *62*, 3657.
(45) Lambert, J.-F.; Poncelet, G. *Top. Catal.* **1997**, *4*, 43.
(46) Stumm, W. *Chemistry of the Solid−Water Interface: Process at the Mineral−Water Interface and Particle−Water Interface in Natural Systems*; J. Wiley & Sons: New York, 1992.
(47) Farley, K. J.; Dzombak, D. A.; Morel, F. M. M. *J. Colloid Interface Sci.* **1985**, *106*, 226.
(48) Danielewicz-Ferchmin, I.; Ferchmin, A. R. *J. Phys. Chem.* **1996**, *100*, 17281.
(49) Danielewicz-Ferchmin, I.; Ferchmin, A. R. *Phys. Chem. Liq.* **2004**, *42*, 1.
(50) Danielewicz-Ferchmin, I.; Ferchmin, A. R. *Phys. Chem. Chem. Phys.* **2004**, *6*, 1332.
(51) Poornachary, S. K.; Chow, P. S.; Tan, R. B. H. *Cryst. Growth Design* **2008**, *8*, 179.
(52) Yang, X.; Lu, J.; Wang, X.-J.; Ching, C.-B. *J. Cryst. Growth* **2008**, *310*, 604.
(53) Poornachary, S. K.; Chow, P. S.; Tan, R. B. H.; Davey, R. J. *Cryst. Growth Design* **2007**, *7*, 254.
(54) Huang, J.; Stringfellow, T. C.; Yu, L. *J. Am. Chem. Soc.* **2008**, *130*, 13973.
(55) Kitadai, N.; Yokoyama, T.; Nakashima, S. *J. Colloid Interface Sci.* **2009**, *329*, 31.
(56) Shelimov, B. N.; Lambert, J.-F.; Che, M.; Didillon, B. *J. Mol. Catal. A* **2000**, *158*, 91.
(57) Bujdák, J.; Rode, B. M. *React. Kinet. Catal. Lett.* **1997**, *62* (2), 281.
(58) Rimola, A.; Ugliengo, P. *Phys. Chem. Chem. Phys.* **2009**, *11*, 2497.

JP906891Y